The Astrophysical Journal, 755:33 (7pp), 2012 August 10 doi:10.1088/0004-637X/755/1/33

COMPOSITION OF THE SOLAR CORONA, SOLAR WIND, AND SOLAR ENERGETIC PARTICLES

J. T. Schmelz[1], D. V. Reames[2], R. von Steiger[3,4], and S. Basu[5]
[1] Physics Department, University of Memphis, Memphis, TN 38152, USA; jschmelz@memphis.edu
[2] IPST, University of Maryland, College Park, MD 20742, USA
[3] ISSI, Hallerstrasse 6, 3012 Bern, Switzerland
[4] Physikalisches Institut, University of Bern, Sidlerstrasse 5, 3012 Bern, Switzerland
[5] Department of Astronomy, Yale University, P.O. Box 208101, New Haven, CT 06520, USA
Received 2012 April 6; accepted 2012 June 7; published 2012 July 24

ABSTRACT

Along with temperature and density, the elemental abundance is a basic parameter required by astronomers to understand and model any physical system. The abundances of the solar corona are known to differ from those of the solar photosphere via a mechanism related to the first ionization potential of the element, but the normalization of these values with respect to hydrogen is challenging. Here, we show that the values used by solar physicists for over a decade and currently referred to as the "coronal abundances" do not agree with the data themselves. As a result, recent analysis and interpretation of solar data involving coronal abundances may need to be revised. We use observations from coronal spectroscopy, the solar wind, and solar energetic particles as well as the latest abundances of the solar photosphere to establish a new set of abundances that reflect our current understanding of the coronal plasma.

Key words: Sun: abundances – Sun: corona – Sun: helioseismology – Sun: particle emission – Sun: photosphere – solar wind

Online-only material: color figures

1. INTRODUCTION

Elemental abundances provide vital clues to the formation of the solar system, the evolution of stars, and the creation of the universe. Because of its proximity and brightness, the Sun has historically been at the forefront of astronomical investigations. It was the main source of the old "cosmic" abundances that were thought to apply to all astronomical objects (Allen 1976). Early hints that this was not the case came at the dawn of the Space Age when rocket-borne instruments began to observe the solar atmosphere and found that cosmic abundances did not apply to the corona.

Abundances determine the opacity of the solar atmosphere and therefore control the heat flow process. They are critical for establishing a host of other solar variables, including temperature and density, because they are a fundamental multiplier in the atomic physics equations for the coronal emission line intensities. The abundance of the trace elements relative to hydrogen (i.e., absolute abundances) in solar plasma is required to deduce the corresponding emission measure, the total amount of emitting material. Abundances affect cooling timescales, energetics, pressure balance, and also determine the shape of the radiative loss function. They are tracers of the origins of the solar system. We can use them to track various components of the solar wind, solar energetic particles (SEPs), and coronal mass ejections back to the solar source.

Coronal abundances are different from their photospheric counterparts. Spectroscopic, SEP, and solar wind data agree that the coronal-to-photospheric abundance ratios of elements with low first ionization potential (FIP $<$ 10 eV) seem to be enhanced relative to those with high FIP ($>$11 eV). This fractionation probably results from a separation of ions and neutrals, which takes place between the photosphere and the corona at temperatures of 6000–10,000 K. Hènoux (1998) suggested that magnetic fields drag the modified mixture up into the corona as active regions develop. Laming (2009) invoked the ponderomotive force in the acceleration of Alfvén waves to create this "FIP effect." Variations of elemental abundances indicate that there is at least one important mechanism that we are not taking into account in our understanding of the solar atmosphere. Absolute coronal abundances are needed to understand the details of this differentiation mechanism.

Since elemental abundances are crucial inputs for these essential physical parameters, it is surprising to learn that the set of values that solar physicists currently refer to as the "coronal abundances" does not agree with the overwhelming majority of spectroscopic, SEP, and solar wind data. These so-called coronal abundances are used everywhere in solar physics, e.g., as the default set in the CHIANTI atomic physics database (Dere et al. 1997; Landi et al. 2012), in models of the response functions for the Solar Dynamics Observatory Atmospheric Imaging Assembly (Boerner et al. 2012), and in one-dimensional hydrodynamic calculations to model coronal loops (Winebarger et al. 2011).

2. ANALYSIS

Jean-Paul Meyer summarized the current state of the coronal abundance problem in two 1985 review papers, one on the baseline composition of SEPs (Meyer 1985a) and the second on solar-stellar outer atmospheres, SEPs, and galactic cosmic rays (Meyer 1985b). Of these results, only one from the rocket data analysis of Veck & Parkinson (1981) was able to present a convincing normalization of the trace elements with respect to hydrogen, a result that is problematic in all abundance analyses.

The culmination of Meyers' extensive review was a set of what he called "adopted coronal" abundances where the values for the low-FIP elements are the same in the corona and the

photosphere while high-FIP elements are depleted by about a factor of four with respect to their photospheric values. Even as the Meyer review papers were coming out, other results were undermining his conclusions. Sylwester et al. (1984) analyzed the coronal calcium-to-hydrogen abundance in solar flares observed with the Bent Crystal Spectrometer (BCS) on board the *Solar Maximum Mission* (*SMM*) satellite. Although the results had large error bars, the flare spectra showed enhancement of low-FIP calcium with respect to its photospheric value. Feldman (1992) used the absolute abundances from these flare data as well as other results for relative abundance to "flip the FIP." He established a new normalization for coronal abundances where low-FIP elements were enhanced by a factor of four with respect to their photospheric values while high-FIP elements were the same in the corona and the photosphere.

With these two different empirical models now in the literature, any evidence for high-FIP depletion was used in support of the Meyer "adopted coronal" abundances. For example, the coronal streamer results of Raymond et al. (1997) used spectroscopic data from the Ultraviolet Coronagraph Spectrometer on the *SOHO* satellite. They found that the abundances for helium, oxygen, and other high-FIP elements were lower than photospheric. At the same time, any evidence of low-FIP enhancement was used in support of the Feldman "FIP-flip" abundances. For example, both Sterling et al. (1993) and Sylwester et al. (1998) found that the absolute abundance of low-FIP Calcium was enhanced.

One additional complicating factor implicated itself in this debate: determining reliable values for the absolute abundances is much more difficult than for relative abundances. In fact, SEP and solar wind data are almost always normalized with respect to oxygen for this reason. Since most of the hydrogen in the corona is ionized and there are essentially no observable spectral lines (however, see Raymond et al. 1997 and Feldman 1998 for notable exceptions), most absolute abundance measurements from coronal spectroscopy require a measurement of the pure continuum, a capacity very few instruments had. As a result, relative abundance measurements were sometime inserted into the Meyer/Feldman debate; unfortunately, the distinction was not always made clear.

2.1. Solar Energetic Particles

The element abundances of SEPs that are most relevant to coronal abundances come from particles accelerated by shock waves driven out from the Sun by coronal mass ejections (e.g., Reames 1999). Particles from these large "gradual" SEP events flow outward along the interplanetary magnetic field to the vicinity of the Earth where we detect, identify, and count each particle directly, rather than counting photons emitted by nuclear or atomic processes near the Sun. Event-averaged element abundances are accumulated for particles at a given velocity (i.e., energy/nucleon), e.g., in the 5–10 MeV amu^{-1} range. One significant advantage of SEP abundances is completeness, in that essentially all elements from H through Zn are measured individually (e.g., Reames 1995, 1998, 1999), with groups of elements measured up through Pb (Reames & Ng 2004).

SEP detection is completely independent of ion atomic properties, while the processes of acceleration and transport can depend upon the mass-to-charge ratio, A/Q, of these highly ionized particles. Event-to-event variations are small for neighboring elements, but larger for widely separated species; abundances averaged over individual events vary by <20% from the mean for Mg/Ne but by a factor of about two for Fe/C (Reames 1995, 1998, 1999). However, these variations become larger below ∼1 MeV amu^{-1} (Desai et al. 2006).

Particles from the smaller "impulsive" SEP events are accelerated in flares or jets, probably by resonant wave–particle interactions (e.g., Temerin & Roth 1992). Here there are large enhancements in ^{3}He/^{4}He and element abundances have a strong dependence on A/Q, such as an average enhancement in Fe/O by an average factor of about eight (Reames 1995, 1998, 1999). These abundance enhancements have been followed up to the vicinity of Pb where they can exceed a factor of ∼1000 (Reames & Ng 2004). Generally, impulsive and gradual events are easily distinguished; however, sometimes the residual suprathermal ions from impulsive SEP events are incorporated into the "seed population" and reaccelerated by a shock, modifying the final abundances (Mason et al. 1999; Tylka et al. 2001, 2005; Desai et al. 2006; Tylka & Lee 2006). The best confirmation that the standard event-averaged abundances for gradual SEP events are relatively free from systematic A/Q bias comes from comparing the abundances of Mg and Si with that of Fe; these elements have similar FIP but different A/Q and they show a similar enhancement relative to photospheric abundances (Reames 1995, 1998, 1999).

Where are SEPs accelerated? For the large events, the shock acceleration can extend over >120 deg in solar longitude. Acceleration begins at about two solar radii near the source longitude. The shock strength decreases with altitude and with longitude away from the source (Reames 2009a, 2009b; Reames & Lal 2010). Acceleration can continue out beyond 1 AU. In fact, below ∼1 MeV/amu most of the SEP ions come from the local plasma near 1 AU, but at higher energies coronal acceleration begins to dominate with reacceleration of those same ions further out. At energies of ∼10 MeV/amu and above, abundances begin to be affected by species-dependent energy-spectral breaks or "knees" in some events. However, high-energy instruments are capable of resolving abundances of isotopes as well as elements (Leske et al. 2007).

Yet another energetic particle population is accelerated at shock waves formed at co-rotating interaction regions (CIRs) where high-speed streams overtake lower-speed solar wind. Particles accelerated by the reverse shock at a CIR, at ∼1–5 AU, flow Sunward toward Earth along the field lines. These energetic ion abundances from CIRs are presumably derived from the tail of distribution function of the high-speed solar wind (Reames 1995, 1999; Mason et al. 2008).

2.2. The Solar Wind

The solar wind plasma, like the SEPs, is accelerated in the solar corona, and thus its composition is expected to agree with that of the corona, not the photosphere. Element abundances in the solar wind can be determined either by the foil collection technique, as used on the *Apollo* missions (Geiss et al. 2004) and, more recently, the *Genesis* mission (Neugebauer et al. 2003), or by in situ mass spectrometry, as used e.g., on the *Ulysses* and *ACE* missions (Gloeckler et al. 1992, 1998). Like the SEPs, solar wind particles are detected, identified, and counted individually and thus yield a more direct measure of its abundances than photons can possibly do. Solar wind abundances are fractionated by the FIP effect, but very little further fractionation due to acceleration processes is expected since these are much more gentle than for SEPs. On the other hand, far fewer elements can be reliably detected in the solar wind than in SEPs or with spectroscopy.

The solar wind is a two-state phenomenon (Geiss et al. 1995), for historical reasons called "fast" and "slow" wind although the two types are better distinguished using the elemental charge state ratios such as O^{7+}/O^{6+} or C^{6+}/C^{5+} (von Steiger et al. 2000). Fast wind emanates from the relatively cool coronal holes and consequently has lower charge states on average than the slow wind, which stems from above the much hotter streamer belt region. The abundances in the two types differ significantly; fast wind is little fractionated by a factor of 2 or less, while the slow wind is more strongly fractionated by a highly variable factor of 2.5 or more, with much higher fractionations occurring predominantly at low heliographic latitudes (von Steiger 2008). Owing to its low variability and FIP fractionation, the fast wind may be considered the closest we can get to photospheric abundances from in situ observations.

A comprehensive list of solar wind abundances based on *Ulysses* observations during 4 300-day periods, 2 each in the fast and slow winds, was published by von Steiger et al. (2000). As usual for most heavy-ion observations, these were relative abundances with respect to oxygen. A subset of them was updated (von Steiger & Zurbuchen 2011) only for fast, coronal hole-associated wind, finding no secular evolution of abundances over the entire *Ulysses* data set of almost two full solar cycles, even though the temperature and other coronal hole properties had evolved remarkably (McComas et al. 2008).

Neon poses a special problem because it is not visible at photospheric temperatures. This has led to conjecture that the discrepancy between helioseismology and the low spectroscopic oxygen abundance might be mended by postulating a higher neon abundance by as much as a factor of three (Bahcall et al. 2005). However, solar wind observations (von Steiger et al. 2000; Bochsler 2007) rule out such a high neon abundance with great confidence because, as already mentioned, the particles can be readily identified individually and a fractionation by more than a factor of two can be excluded in the fast solar wind. This result is supported by coronal spectroscopy—the neon-to-oxygen abundance ratio in both active regions (Schmelz et al. 2005) and the quiet Sun (Young 2005) agrees with the photospheric value. It appears that the discrepancy between helioseismology and the low photospheric oxygen abundance cannot be explained with a higher neon abundance (see Section 2.4 for more details).

2.3. The Solar Corona

Fludra & Schmelz (1999) realized that the coronal abundance normalization did not have to be purely "adopted coronal" or purely "FIP-flip"—that some combination of both models would give a more accurate picture of the coronal plasma, with both low-FIP enhancement and high-FIP depletion, but neither by as great as a factor of four. Their paper summarized all coronal spectroscopic and SEP results where elemental abundances could be normalized with respect to hydrogen. A plot similar to their Figure 4 is shown here in Figure 1(a), where the coronal-to-photospheric elemental abundance ratios as a function of FIP. The SEP and CIR data from Reames (1995) were renormalized with respect to hydrogen and displayed as blue stars and diamonds, respectively. The spectroscopic measurements from Veck & Parkinson (1981), Sterling et al. (1993), Sylwester et al. (1998), and Fludra & Schmelz (1999) are plotted as black symbols. All values were normalized to the photospheric abundances of Grevesse & Anders (1989). These data show conclusively that the composition of coronal plasma and the particle populations is significantly different from that of the solar photosphere.

Figure 1 also shows the two competing empirical models. The upper dashed line represents the Feldman (1992) "FIP-flip" abundances and the lower dashed line represents the Meyer (1985b) "adopted coronal" abundances. The results indicated that neither model did a good job of representing the actual data. This disagreement led Fludra & Schmelz (1999) to propose a "hybrid" abundance normalization. They took a weighted mean of all the low-FIP (2.1 ± 0.7) and the high-FIP (0.65 ± 0.22) data points in Figure 1(a) and multiplied the photospheric abundances by the resulting values. The "hybrid abundance" model is shown as the middle dashed line in Figure 1. These results are summarized in the left half of Table 1, which lists the element, the FIP, the photospheric abundances of Grevesse & Anders (1989), the hybrid abundances of Fludra & Schmelz (1999), and the hybrid-to-photospheric ratio. Although these results have been in the literature for over a decade, the solar physics community has chosen instead to adopt the "FIP flip" abundance model of Feldman (1992).

2.4. A Firm Foundation?

The FIP effect on coronal abundances was built on what we thought was a firm foundation, i.e., the photospheric abundances. That foundation, however, has gone from solid bedrock to shifting sands as new three-dimensional hydrodynamic models (Allende Prieto et al. 2001; Asplund et al. 2000) have been used to determine solar abundances. These models account for temperature and velocity fields associated with convection. Additionally, these calculations of abundances relax the assumption of local thermodynamic equilibrium used to compute atomic level populations. When these results were applied to solar absorption lines, the photospheric abundances that once seemed entrenched (Allen 1976) began to shift. The oxygen abundance, for example, has plummeted from a high of 8.93 ± 0.04 (Grevesse & Anders 1989) to a low of 8.66 ± 0.05 (Asplund et al. 2005). This fall of almost a factor of two is shown in Figure 2. Other light elements (carbon, nitrogen) and the noble gasses (neon, argon), whose photospheric abundances were often tied to oxygen, fell too. The high-FIP end of the coronal abundance diagram in Figure 1(a) had to be redrawn.

These new abundances, however, were challenged by the helioseismology community whose measurements were so precise that they could determine the depth of the solar convection zone, the abundance of helium in the convection zone, as well as subtle features associated with the ionization of heavy elements. Helioseismologists showed that the standard solar model agreed so well with the Sun that it could rule out astrophysical solutions of the solar neutrino problem. This agreement between theory and observation was the envy of all astrophysics—until the metal content of the Sun was reduced by 30% (Asplund et al. 2005). These elements provide a major source of opacity for the solar interior, which determines the internal solar structure and the depth of the convection zone. Models constructed with the lower abundances also had a much lower convection-zone helium abundance than the Sun. The changes were significant enough to shatter the harmonious agreement between theory and observation that had come to exemplify scientific progress. The discrepancies between the two far exceed either the observational uncertainties or the model predictions (Bahcall et al. 2006).

Helioseismic analyses raised the question whether the new abundance analysis was incorrect or whether some inputs to standard solar models, such as opacities and diffusion rates,

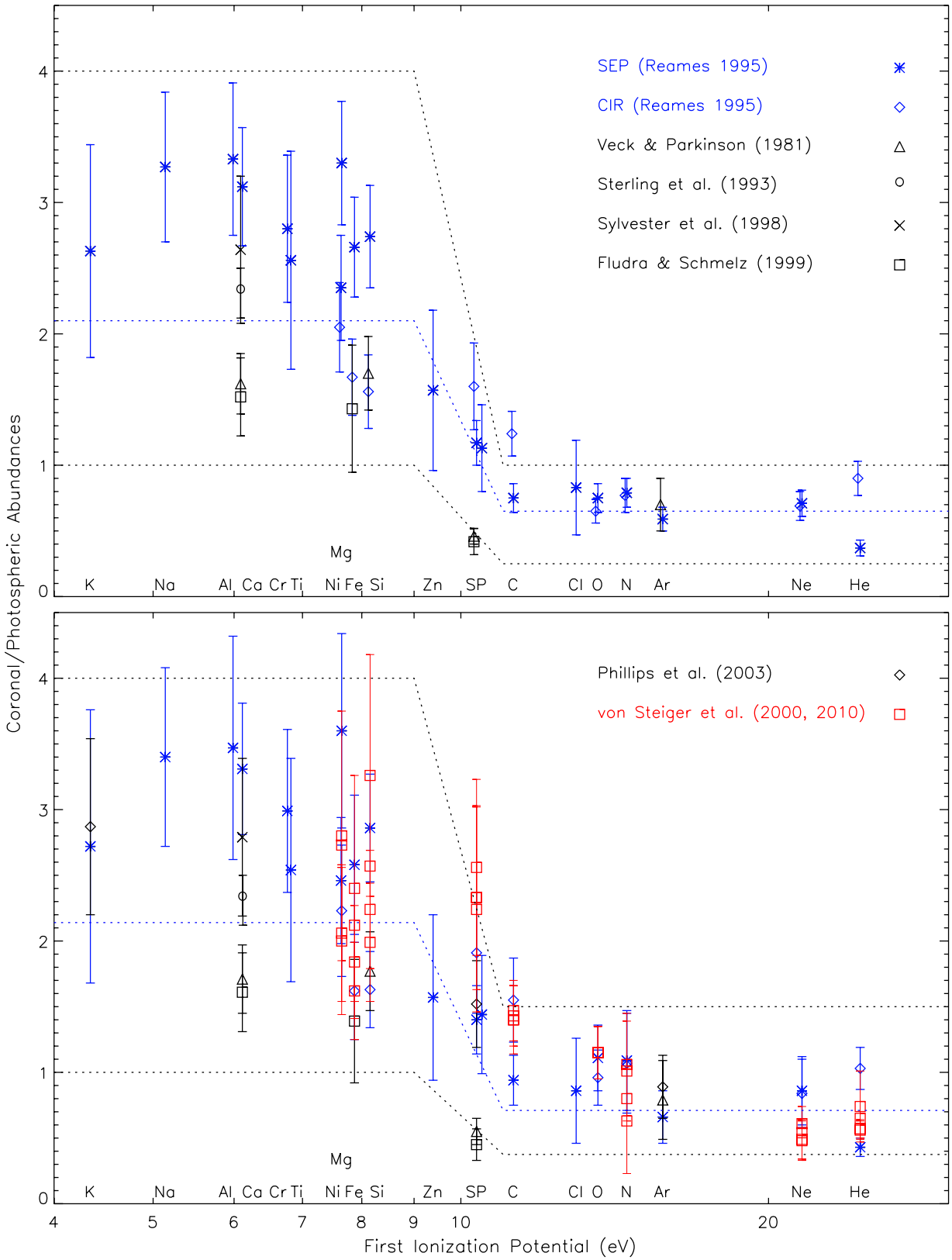

Figure 1. Coronal/photospheric elemental abundances as a function of FIP. The dashed lines represent the two empirical models: upper is low-FIP abundance enhancement (Feldman 1992) and lower is high-FIP depletion (Meyer 1985b) with respect to photospheric values. We also plot the best fit to the data (middle). Results from particle analysis are shown in blue, coronal spectroscopy in black, and solar wind in red. Each data point represents many events/measurements from 25 to several hundred. The upper panel normalizes the coronal abundances with respect to photospheric values of Grevesse & Anders (1989); lower panel uses the modern equivalents from Caffau et al. (2011) and Lodders et al. (2009).

(A color version of this figure is available in the online journal.)

Table 1
Recommended Abundances for the Solar Corona[a]

	FIP (eV)	Anders & Grevesse'89	Hybrid '99 Abundances	Hybrid/ G&A	Caffau & Lodders	SEP Reames'95	Recommended Abundances	Coronal/ C&L
K	4.341	1.33e-7	2.79e-7	2.1	1.29e-7	3.50e-7	2.75e-7	2.14
Na	5.139	2.03e-6	4.25e-6	2.1	1.95e-6	6.62e-6	4.17e-6	2.14
Al	5.986	3.00e-6	6.30e-6	2.1	2.88e-6	1.00e-5	6.16e-6	2.14
Ca	6.113	2.16e-6	4.54e-6	2.1	2.04e-6	6.75e-6	4.36e-6	2.14
Cr	6.766	4.77e-7	1.00e-6	2.1	4.47e-7	1.34e-6	9.55e-7	2.14
Ti	6.82	8.47e-8	1.78e-7	2.1	8.51e-8	2.17e-7	1.82e-7	2.14
Ni	7.635	1.74e-6	3.65e-6	2.1	1.66e-6	4.08e-6	3.55e-6	2.14
Mg	7.646	3.78e-5	7.94e-5	2.1	3.47e-5	1.25e-4	7.41e-5	2.14
Fe	7.87	3.21e-5	6.74e-5	2.1	3.31e-5	8.54e-5	7.08e-5	2.14
Si	8.151	3.53e-5	7.42e-5	2.1	3.39e-5	9.68e-5	7.24e-5	2.14
Zn	9.394	4.45e-8	8.05e-8	1.81	4.47e-8	7.01e-8	8.26e-8	1.85
S	10.36	1.73e-5	1.97e-5	1.14	1.45e-5	2.03e-5	1.69e-5	1.17
P	10.49	3.67e-7	3.74e-7	1.02	2.88e-7	4.14e-7	3.09e-7	1.07
C	11.26	3.97e-4	2.57e-4	0.65	3.16e-4	2.96e-4	2.26e-4	0.71
Cl	12.97	1.85e-7	1.20e-7	0.65	1.78e-7	1.53e-7	1.27e-7	0.71
O	13.62	8.47e-4	5.48e-4	0.65	5.75e-4	6.37e-4	4.11e-4	0.71
N	14.53	1.00e-4	6.47e-5	0.65	7.24e-5	7.90e-5	5.17e-5	0.71
Ar	15.76	3.57e-6	2.31e-6	0.65	3.16e-6	2.10e-6	2.26e-6	0.71
Ne	21.56	1.36e-4	8.83e-5	0.65	1.12e-4	9.68e-5	8.01e-5	0.71
He	24.59	9.75e-2	6.31e-2	0.65	8.51e-2	3.63e-2	6.08e-2	0.71

Note. [a] The notation e-4 means 10∧(-4) (not the natural exponential function).

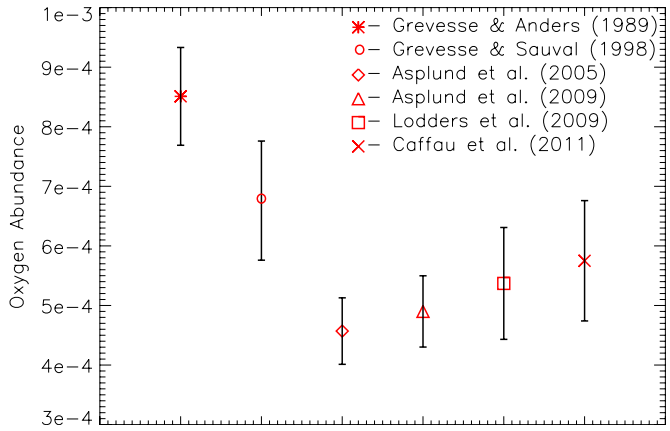

Figure 2. Recent evolution of the photospheric abundance of oxygen, which was falling and is now rebounding. The photospheric abundances of other light elements (carbon, nitrogen) and the noble gasses (neon, argon) are often tied to oxygen, so this change affected the high-FIP end of the coronal abundance diagram shown in Figure 1.

(A color version of this figure is available in the online journal.)

were incorrect. To get solar models with low metallicity up to par with observation again would require finely tuned changes in opacities, diffusion rates, as well as the equation of state (Basu & Antia 2008). Other proposed solutions included late accretion on to the Sun (Guzik & Mussack 2010; Serenelli et al. 2011), but these were not completely satisfactory either.

Figure 2 shows how the photospheric oxygen abundance has continued to change. Asplund et al. (2009) revised the Asplund et al. (2005) results upward to 8.69 ± 0.05, and other groups have challenged these results. Using a different three-dimensional atmospheric model and a different set of spectral lines, Caffau et al. (2011) claim a solar oxygen abundance of 8.76 ± 0.07. Since the accepted photospheric abundances for most of the high-FIP elements scale with oxygen, the foundation of the FIP model and the normalization of the coronal abundances had to be changed as well.

3. DISCUSSION

For this work we choose to adopt the photospheric abundances of Caffau et al. (2011). Our choice is based not only on the fact that this is the most recent abundance determination, but also because standard solar models constructed with the Caffau et al. (2011) abundances match helioseismic constraints quite well (Antia & Basu 2011). The sound-speed profile, the density profile, as well as the convection-zone helium abundance of these models are as good as the higher-Z models that were used to rule out astrophysical solutions of the solar neutrino problem. The meteoritic abundance values from Lodders et al. (2009) are used for elements not included in the Caffau et al. (2011) analysis.

The current absolute abundance data from coronal spectroscopy, SEPs, and the solar wind are included in Figure 1(b). We have added new spectroscopy results for RESIK (Phillips et al. 2003), an instrument similar to the BCS on *SMM* and on *Yohkoh*. Also now available are absolute abundance results for the solar wind from von Steiger et al. (2000, 2010). These were obtained by comparing the absolute flux of oxygen from SWICS with the absolute proton flux from SWOOPS on *Ulysses* giving a value of 8.82 ± 0.08. The solar wind data for different elements were renormalized to hydrogen using this absolute abundance of oxygen and are plotted as red squares in Figure 1(b). All the data points as well as the empirical models of Meyer (1985b) and Feldman (1992) are now normalized to the photospheric abundances of Caffau et al. (2011) and Lodders et al. (2009).

The abundance variations seen in Figure 1 (as a function of FIP, from element to element, from one instrument to another for the same element) cannot be explained using statistical uncertainties alone. It is also unlikely that actual abundance variability from region to region can account for the seemingly discrepant data. One reality that we are forced to confront is the difficulty in determining a convincing normalization of the trace elements with respect to hydrogen, a result that is problematic in all abundance analyses. In our attempt to

Table 2
Coronal Spectroscopy Results for Iron

Abundance[a]	Instrument	Target	Reference
1.56e-4	*SOHO* CDS-VLA	Active Region	White et al. (2000)
1.26e-4	*SOHO* SUMER	Streamer	Feldman (1998)
8.13e-5	*RHESSI*	Flares	Phillips et al. (2012)
7.80e-5	*SOHO* EIT-VLA	Full Sun	Zhang et al. (2001)
6.74e-5	*Hinode* XRT-*RHESSI*	Active Region	Schmelz et al. (2009)
6.62e-5	*Yohkoh* BCS	Flares	Phillips et al. (1994)
6.62e-5	*Hinode* EIS-XRT	Active Region	Testa et al. (2011)
4.60e-5	*Yohkoh* BCS	Flares	Fludra & Schmelz (1999)
3.16e-5	*SOHO* UVCS	Streamer	Raymond et al. (1997)

Note. [a] The notation e-4 means 10∧(-4) (not the natural exponential function).

determine a recommended set of coronal abundances, how can we either account for or address the systematic uncertainties that appear to dominate our analysis?

For SEPs, factor-of-two variations are seen in the H/He abundance ratio, which can also show significant energy dependence. Hence the absolute normalization of SEP abundances to hydrogen is much less certain than the relative abundances of other elements. For the solar wind, it is difficult to measure absolute abundances with in situ mass spectrometry because protons are so much more abundant than all heavy ions. Therefore, it is necessary to measure protons in a different instrument mode or even with a different sensor, thus raising issues of intercalibration and other systematic uncertainties.

An interesting insight into the nature of these systematic uncertainties is provided by results from coronal spectroscopy for the absolute abundance of iron. Table 2 shows the iron abundance, instrument, solar source, and reference. These data span the range from Meyer (1985b) to Feldman (1992), raising the question of just how well we can measure these absolute abundances. Instrument cross-calibration, target selection, and an uncontaminated measurement of the continuum all play a role in the seemingly discrepant results, and it is not clear which (if any) of the values are wrong.

For example, the highest iron abundance comes from the comparison of *SOHO* CDS iron lines and thermal bremsstrahlung emission from the hydrogen continuum measured by the Very Large Array (VLA; White et al. 2000). This EUV–radio comparison showed great promise, but a similar analysis *by the same group* using one of the *SOHO* EIT iron channels and the VLA thermal bremsstrahlung emission resulted in an absolute iron abundance that agreed with the hybrid value (Zhang et al. 2001). These results relied heavily on the CDS-VLA or EIT-VLA cross-calibration. Strictly speaking, it is easier to cross-calibrate full disk instruments so one might be tempted to put more credence in the lower EIT result. There is, however, no way to tell which cross-calibration was right (or even which one was better).

The second highest iron abundance in Table 2 is for the *SOHO* SUMER streamer from Feldman (1998). The hydrogen measurements come from Lyβ. The lowest value in the table, however, also comes from a streamer result. *SOHO* UVCS provides Lyα measurements for hydrogen (Raymond et al. 1997). It is worth noting that Feldman et al. also measured a declining iron abundance with height (at least as compared with silicon), and that this trend is consistent with the UVCS value. The amount of gravitational settling that occurs as we move to different levels of the solar atmosphere is probably the biggest factor in trying to account for these differences.

The other low iron abundance result in Table 2 is the *Yohkoh* BCS value for solar flares from Fludra & Schmelz (1999). Here, the iron line fluxes are paired with a measure of the continuum to get absolute abundances. The crucial factor in this analysis is that the continuum emission must not contain any instrumental contamination (although a combination of thermal bremsstrahlung, free-bound, and two-photon emission is fine). The *SMM* BCS results of Sylwester et al. (1998) did not include iron, but both *SMM* BCS and *Yohkoh* BCS measured calcium, and the *Yohkoh* BCS results were systematically lower. This difference was often attributed to (and is consistent with) instrumental contamination in the *Yohkoh* BCS. The other relevant comparison, however, is with *Yohkoh* BCS and the OSO-8 graphite crystal spectrometer results of Veck & Parkinson (1981). Both measured the absolute calcium abundance, but the graphite crystal gave a much better observation of the continuum than either of the BCS instruments. As we see from Figure 1, it is the *Yohkoh* BCS results that agree with those of Veck & Parkinson (1981); the *SMM* BCS coronal calcium results are significantly higher. Once again, there is no way to tell which result, if either, we should adopt, at least not without a detailed laboratory examination of the instruments, which, of course, is not possible.

These results indicate that we should be cautious in using any one measurement or any measurements from one instrument as *the* value supporting *the* model of coronal abundances. It is reassuring, however, that the five middle entries for the iron abundance in Table 2, the *RHESSI* flares (Phillips et al. 2012), the *SOHO* EIT-VLA observations (Zhang et al. 2001), the *Hinode* XRT-*RHESSI* results (Schmelz et al. 2009), the *Yohkoh* BCS flares (Phillips et al. 1994), and the *Hinode* EIS-XRT active region data (Testa et al. 2011) are all within 1σ of the old hybrid result for iron from Fludra & Schmelz (1999). It is also encouraging that the average of all the diverse values for the absolute abundance of iron listed in Table 2 is $7.99 \pm 3.86 \times 10^{-5}$, which also agrees with the hybrid value.

The goal of this paper is to establish a recommended set of abundances for the solar corona, which is based on the available absolute abundances determined from SEP, solar wind, and spectroscopy data. In light of the discussion above on systematic uncertainties and the encouraging agreement of recent iron abundance results (Table 2) with the Fludra & Schmelz (1999) hybrid iron value, we have elected to follow the procedure used by Fludra & Schmelz.

We begin with the low-FIP elements, which includes potassium through silicon. Figure 1(b) shows 32 low-FIP data points; the weighted mean of these coronal-to-photospheric ratios is 2.14 ± 0.46. The middle dashed line on the low-FIP side of Figure 1(b) represents this value. We follow the same procedure

for the high-FIP elements, which includes carbon through helium. Figure 1(b) shows 34 low-FIP data points; the weighted mean of these coronal-to-photospheric ratios is 0.71 ± 0.14. The middle dashed line on the high-FIP side of Figure 1(b) represents this value. For the intermediate-FIP elements, we simply connect the low-FIP and high-FIP values with a straight line (please see Figure 1(b)).

Finally, to determine our set of recommended abundances for the solar corona, we multiply the low-FIP photospheric abundances by 2.14, the high-FIP photospheric abundances by 0.71, and interpolate for the intermediate-FIP elements. Our results are summarized in the right half of Table 1, which list the photospheric abundances from Caffau et al. (2011) and Lodders et al. (2009), our recommended set of coronal abundances determined from this technique, and the ratios from the weighted means. The old hybrid abundances and the SEP values are listed for comparison.

Although Figure 1(b) clearly shows that it is impossible to provide a single model satisfying all observations, and although it is vital to account for the possibility of abundance variability, it is often useful to begin new research projects with a set of abundances. Our results, which include research from several groups using various types of data from different instruments on numerous spacecrafts, show conclusively that this set should be the "Recommended Abundances" listed in Table 1. We propose that these abundances be used as the default values in future investigations.

We thank K. Strong for critical discussions, Y. Strong for reading an early version of this manuscript, and J. Kimble and B. Jenkins for assistance with figures.

REFERENCES

Allen, C. W. 1976, Astrophysical Quantities (London: Athlone)
Allende Prieto, C., Lambert, D. L., & Asplund, M. 2001, ApJ, 556, L63
Antia, H. M., & Basu, S. 2011, J. Phys.: Conf. Ser., 271, 012034
Asplund, M., Grevesse, N., & Sauval, A. J. 2005, in ASP Conf. Ser. 336, Cosmic Abundances as Records of Stellar Evolution and Nucleosynthesis, ed. T. G. Barnes & F. N. Bash (San Francisco, CA: ASP), 25
Asplund, M., Grevesse, N., Sauval, A. J., & Scott, P. 2009, ARA&A, 47, 481
Asplund, M., Nordlund, A., Trampedach, R., & Stein, R. F. 2000, A&A, 359, 743
Bahcall, J. N., Basu, S., & Serenelli, A. M. 2005, ApJ, 631, 1281
Bahcall, J. N., Serenelli, A. M., & Basu, S. 2006, ApJS, 165, 400
Basu, S., & Antia, H. M. 2008, Phys. Rep., 457, 217
Bochsler, P. 2007, A&A, 471, 315
Boerner, P., Edwards, C., Lemen, J., et al. 2012, Sol. Phys., 275, 41
Caffau, E., Ludwig, H.-G., Steffen, M., Freytag, B., & Bonofacio, P. 2011, Sol. Phys., 268, 255
Dere, K. P., Landi, E., Mason, H. E., Monsignori Fossi, B. C., & Young, P. R. 1997, A&AS, 125, 149
Desai, M. I., Mason, G. M., Gold, R. E., et al. 2006, ApJ, 649, 740
Feldman, U. 1992, Phys. Scr, 46, 202
Feldman, U. 1998, Space Sci. Rev., 85, 27
Fludra, A., & Schmelz, J. T. 1999, A&A, 348, 286
Geiss, J., Bühler, F., Cerutti, H., et al. 2004, Space Sci. Rev., 110, 307
Geiss, J., Gloeckler, G., & von Steiger, R. 1995, Space Sci. Rev., 72, 49
Gloeckler, G., Cain, J., Ipavich, F. M., et al. 1998, Space Sci. Rev., 86, 497
Gloeckler, G., Geiss, J., Balsiger, H., et al. 1992, A&AS, 92, 267
Grevesse, N., & Anders, E. 1989, in AIP Conf. Ser. 183, Cosmic Abundances of Matter (Melville, NY: AIP), 1
Guzik, J. A., & Mussack, K. 2010, ApJ, 713, 1108
Hènoux, J.-C. 1998, Space Sci. Rev., 85, 215
Landi, E., Del Zanna, G., Young, P. R., Dere, K. P., & Mason, H. E. 2012, ApJ, 744, 99
Laming, J. M. 2009, ApJ, 695, 954
Leske, R. A., Mewaldt, R. A., Cohen, C. M. S., et al. 2007, Space Sci. Rev., 130, 195
Lodders, K., Palme, H., & Gail, H. P. 2009, in Landolt-Börnstein, New Series, Vol. VI/4B, ed. J. E. Trümper (Berlin: Springer), 560, Chap. 4.4
Mason, G. M., Leske, R. A., Desai, M. I., et al. 2008, ApJ, 678, 1458
Mason, G. M., Mazur, J. E., & Dwyer, J. R. 1999, ApJ, 525, L133
McComas, D. J., Ebert, R. W., Elliott, H. A., et al. 2008, Geophys. Res. Lett., 35, 5
Meyer, J.-P. 1985a, ApJS, 57, 151
Meyer, J.-P. 1985b, ApJS, 57, 173
Neugebauer, M., Steinberg, J. T., Tokar, R. L., et al. 2003, Space Sci. Rev., 105, 661
Phillips, K. J. H., Pike, C. D., Lang, J., Watanbe, T., & Takahashi, M. 1994, ApJ, 435, 888
Phillips, K. J. H., Sylwester, J., Sylwester, B., & Landi, E. 2003, ApJ, 589, L113
Phillips, K. J. H., & Dennis, B. R. 2012, ApJ, 748, 52
Raymond, J. C., Kohl, J. L., Noci, G., et al. 1997, Sol. Phys., 175, 645
Reames, D. V. 1995, Adv. Space Res., 15, 41
Reames, D. V. 1998, Space Sci. Rev., 85, 327
Reames, D. V. 1999, Space Sci. Rev., 90, 413
Reames, D. V. 2009a, ApJ, 693, 812
Reames, D. V. 2009b, ApJ, 706, 844
Reames, D. V., & Lal, N. 2010, ApJ, 723, 550
Reames, D. V., & Ng, C. K. 2004, ApJ, 610, 510
Schmelz, J. T., Kashyap, V. L., Saar, S. H., et al. 2009, ApJ, 704, 863
Schmelz, J. T., Nasraoui, K., Roames, J. K., Lippner, L. A., & Garst, J. W. 2005, ApJ, 634, L197
Serenelli, A. M., Haxton, W. C., & Peña-Garay, C. 2011, ApJ, 743, 24
Sterling, A. C., Doschek, G. A., & Feldman, U. 1993, ApJ, 404, 394
Sylwester, J., Lemen, J. R., Bentley, R. D., Fludra, A., & Zolcinski, M.-C. 1998, ApJS, 501, 397
Sylwester, J., Lemen, J. R., & Mewe, R. 1984, Nature, 310, 665
Temerin, M., & Roth, I. 1992, ApJ, 391, L105
Testa, P., Reale, F., Landi, E., DeLuca, E. E., & Kashyap, V. 2011, ApJ, 728, 30
Tylka, A. J., Cohen, C. M. S., Deitrich, W. F., et al. 2001, ApJ, 558, L59
Tylka, A. J., Cohen, C. M. S., Dietrich, W. F., et al. 2005, ApJ, 625, 474
Tylka, A. J., & Lee, M. A. 2006, ApJ, 646, 1319
Veck, N. J., & Parkinson, J. H. 1981, MNRAS, 197, 41
von Steiger, R. 2008, The Solar Wind throughout the Solar Cycle, in The Heliosphere through the Solar Activity Cycle, ed. A. Balogh, L. J. Lanzerotti, & S. Suess (Berlin: Springer Praxis Books), 41
von Steiger, R., Schwadron, N. A., Fisk, L. A., et al. 2000, J. Geophys. Res., 105, 27217
von Steiger, R., & Zurbuchen, T. H. 2011, J. Geophys. Res., 116, 1105
von Steiger, R., Zurbuchen, T. H., & McComas, D. J. 2010, Geophys. Res. Lett., 37, 22101
White, S. M., Thomas, R. J., Brosius, J. W., & Kundu, M. R. 2000, ApJ, 534, 203
Winebarger, A. R., Schmelz, J. T., Warren, H. P., Saar, S. H., & Kashyap, V. L. 2011, ApJ, 740, 2
Young, P. R. 2005, A&A, 444, 45
Zhang, J., Kundu, M. R., White, S. M., Dere, K. P., & Newmark, J. S. 2001, ApJ, 561, 396